Thermal Decomposition of an Ultrathin Si Oxide Layer around a Si(001)-(2 × 1) Window

Noriyuki Miyata, Heiji Watanabe,* and Masakazu Ichikawa

Joint Research Center for Atom Technology, Angstrom Technology Partnership (JRCAT-ATP), c/o National Institute for Advanced Interdisciplinary Research (NAIR), 1-1-4 Higashi, Tsukuba, Ibaraki 305-0046, Japan

(Received 13 July 1999)

We examine the thermal decomposition of an ultrathin Si oxide layer around a Si(001)-(2 × 1) window opened by electron-beam-induced selective thermal decomposition. The decomposition progresses at the oxide/Si(001)-(2 × 1) boundary and follows two rate-limiting steps with activation energies of 4.0 and 1.7 eV. We propose that the former and latter energies correspond to the reaction of Si monomer with the oxide and the desorption of the SiO into the vacuum, respectively.

PACS numbers: 82.30.Lp, 68.35.Bs, 81.65.Cf, 81.65.Mq

An ultrathin Si oxide layer thermally grown on a Si surface is one of the most important structures in the microelectronic devices. For example, oxide layers that are less than 3-nm thick have already been employed as gate dielectric layers in metal-oxide-semiconductor (MOS) devices, and a nanometer-scale mask using an ultrathin oxide layer (<1 nm) has been developed for future fabrication technology [1,2]. A large number of studies have been done on the thermal decomposition of the thin Si-oxide layers, because the thermally induced defects around the SiO_2/Si interface is the key issue to achieving good electrical reliability in MOS devices [3]. In addition, the thermal stability of the ultrathin oxide mask is also crucial for the production of a fine nanometer-scale structure [4].

Tromp *et al.* reported that the thermal decomposition of the oxide layer (~10 nm) by ultrahigh-vacuum (UHV) annealing is a spatially inhomogeneous reaction in which the holes with a clean Si surface are initially formed, and then the decomposition progresses with the SiO desorption at the edge of the hole ($SiO_2 + Si \rightarrow 2SiO\uparrow$) [5]. They showed that the decomposition of an ultrathin Si-oxide layer (<1 nm) occurs in a similar inhomogeneous manner [6–8]. Therefore, the important reaction is thought to occur around the oxide/Si boundary. In addition, the SiO desorption under low-oxygen pressure at high temperature or at the submonolayer region have been energetically investigated [9–15]. However, the mechanism of the oxide decomposition is still not fully understood. In particular, the activation energy E_d has been reported to fall in a wide range of energies (~1.5–4.0 eV) [6,9–16], and the reaction step of E_d has not been clearly determined. On the other hand, Fujita *et al.* recently reported that a nanometer-scale clean Si window can be intentionally opened in an ultrathin Si-oxide layer (<1 nm) by using an electron-beam-induced selective thermal decomposition (EB-STD) [2]. This Si-oxide mask provides us with a unique way of investigating the reaction around the oxide/Si(001)-(2 × 1) boundary. In the current research, we used scanning reflection electron microscopy (SREM) to observe the structural change around a Si(001)-(2 × 1) window opened by EB-STD and discussed the rate limiting step of the oxide decomposition.

Sample preparation and surface observation were carried out by using an UHV surface-analysis system [17]. The samples, which were 2.5 × 15 × 0.5 mm, were cut from an *n*-type Si(001) wafer. The atomically flat Si(001)-(2 × 1) surfaces were prepared by flash heating at 1200 °C under UHV conditions. Four types of ultrathin Si-oxide layers were then thermally grown under the following oxidation conditions: 1×10^{-6} Torr O_2 pressure at 470 °C for 10 min, 2×10^{-6} Torr O_2 pressure at 650 °C for 10 min, 2×10^{-6} Torr O_2 pressure at 725 °C for 5 min, 5×10^{-5} Torr O_2 pressure at 800 °C for 1 min. X-ray photoelectron spectroscopy (XPS) measurement determined the thicknesses of all oxide layers to be about 0.3 nm [4]. The SREM observations of the oxide layers indicated that the interfaces were atomically flat and showed the reversion of terrace contrast. These results indicate that the one-atomic-layer Si on the Si(001)-(2 × 1) surface was oxidized under these oxidation conditions [18]. The Si(001)-(2 × 1) open windows were formed by irradiation with a focused 30-keV EB that had a diameter of about 3 nm and successive thermal annealing at 720 °C for 3–10 min [2]. We used Si(001)-(2 × 1) linear open windows with width of 15–50 nm. The samples were annealed at a pressure of less than 2×10^{-10} Torr.

SREM observation was performed at room temperature. The reflection high-energy electron diffraction (RHEED) pattern on a fluorescent screen was observed by using a 30-keV EB with a 3-nm diameter. The SREM images were obtained by monitoring a specular spot with a glancing angle of about 2°. The chemical structures of the as-grown oxide layers were evaluated by using XPS with Mg $K\alpha$ x-ray radiation [4]. In addition, the compositional change after the UHV annealing was investigated by using microprobe Auger electron spectroscopy (μ-AES).

The SREM image shown in Fig. 1(a) shows an initial Si(001)-(2 × 1) linear window with a width of about 21 nm that was opened in the 650 °C oxide layer. The bright and dark regions correspond to the Si(001)-(2 × 1) and the oxide-covered surfaces, respectively. The SREM image in Fig. 1(b) shows the same Si(001)-(2 × 1) window after annealing at 700 °C for 13 min. The width of the Si window, as estimated from the profile of the SREM

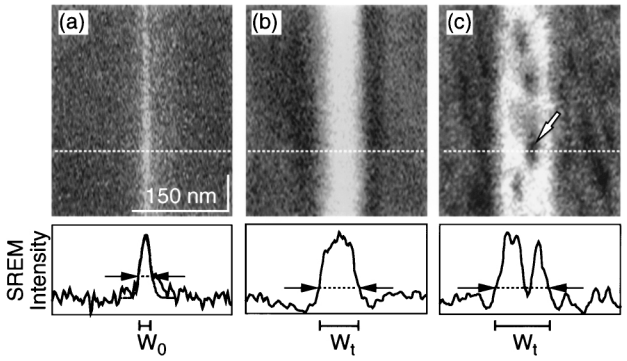

FIG. 1. Scanning reflection electron microscopy images. (a) Initial Si(001)-(2 × 1) open window formed in the ultrathin oxide layer. Si window annealed at 700 °C for 13 min (b) and 20 min (c).

intensity, increased after the annealing. Further annealing at the same temperature widened the Si window [Fig. 1(c)]. Similar SREM results were obtained at other annealing temperatures and for the other temperature-oxide layers. These results indicate that the oxide at the oxide/Si boundary was removed by the thermal decomposition.

Dark patches also appeared in the Si(001)-(2 × 1) window [Fig. 1(c)]. By using μ-AES, we confirmed that these images were not caused by contamination by elements such as oxygen and carbon. In addition, we used profile analysis of RHEED [19] to evaluate the atomic-scale roughness of the Si windows. We observed the (10) spot from the Si window during the annealing at 700 °C and found that the streak intensity increased with the annealing. This result indicates that the thermal decomposition accompanies the formation of the atomic-scale roughness on the Si window surface. Comparing the measured and calculated (10)-spot profiles by using diffraction theory, we estimated the island size to be about 10 nm. This size is roughly consistent with the SREM image of Fig. 1(c). The increase of atomic-scale roughness suggests that the Si atoms on the Si window surface were consumed during the oxide decomposition.

Figure 2 shows the change in the window width, $W_t - W_0$, for the 650 °C-oxide mask as a function of annealing time. W_0 is the width of the initial Si linear window and W_t is the width after annealing for t min. The closed and opened circles in the lower part of Fig. 2 show the widening property for the 650 °C-oxide mask annealed at 700 and 630 °C, respectively. The solid lines in Fig. 2 indicate that the widths increase linearly with the annealing time. We defined the decomposition rate to be the slope of this linear region. The triangular plots in the upper part of Fig. 2 are the normalized O_{KLL} intensities obtained from the oxide-covered surface detached from the Si(001)-(2 × 1) windows. The oxide layer was stable, even when the oxide decomposition progressed around the Si window. This result indicates that the decomposition occurs only at the oxide/Si boundary. However, when we continue the

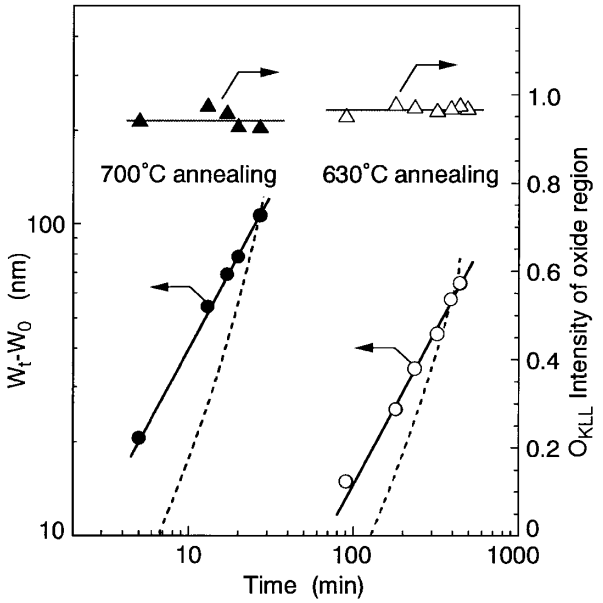

FIG. 2. The dependence of window width, $W_t - W_0$, and O_{KLL} intensity on the annealing time. W_0 is the width of the initial Si(001)-(2 × 1) linear window and W_t is the width annealed for t minutes. The O_{KLL} intensities were normalized by that of the initial oxide surface.

annealing for longer times, the O_{KLL} intensity decreased because voids with clean Si surface are formed in the oxide layer [7,8]. In this work, we focus on the reaction at the oxide/Si boundary before void formation in the oxide layer occurs.

Our results indicate that the decomposition progresses only at the oxide/Si boundary. In addition, the consumption of Si atoms on the Si window surface suggests that the mobile Si monomer produced on the Si surface reacts with the oxide. The reaction is a follow-four-step process that is similar to the previously proposed void expansion process in ultrathin Si-oxide layers [7]. First, the Si monomer is produced on the Si window surface. Second, the Si monomer migrates on the Si surface until it arrives at the oxide/Si boundary. Third, the Si monomer reacts with the Si oxide to form a precursor structure like a SiO adsorbate. Finally, volatile SiO desorbs into the vacuum. Now let us discuss the rate-limiting step in terms of this reaction mechanism. If we consider the reaction (1) to be the limiting step, the decomposition rate dW/dt depends on the area of Si window. Because we can neglect the change in the length of the Si linear window, dW/dt can be written as

$$\frac{dW}{dt} \propto W . \tag{1}$$

This relationship indicates that W increases exponentially with annealing time, as shown by dotted curves in Fig. 2. It is obvious that these fitting curves are not consistent with the measured data. It should be noted that the ability for

producing the Si monomer on the Si(001)-(2 × 1) surface may depend on the degree of atomic-scale roughness on the Si window surface. It was reported that, during the void formation in the ultrathin Si oxide layer, the Si monomer was preferentially detached from the atomic steps on the off-axis Si(001) surface [20], so it would be expected that an atomically rough Si surface is more capable of supplying the Si monomer compared with an atomically flat surface. Therefore, the rate of reaction (1) is thought to increase with annealing, and it can be expected that the decomposition curves part from the measured data still more. Judging from the above discussion, reaction (1) is not the rate-limiting step.

Figure 3 shows the Arrhenius plot of the decomposition rate of various oxide layers. We can recognize the two linear regions in the decomposition property of the 650 °C oxide layer, so there are at least two dominant reactions. By assuming that the reactions in these two regions follow Arrhenius forms independently of each other, the E_d of the higher (>700 °C) and that of the lower (<700 °C) temperature regions were estimated to be 1.7 and 4.0 eV, respectively. The plots for the other oxide layers also indicated E_d to be 1.7 or 4.0 eV. It is obvious that these two activation energies are higher than that of the migration of the Si monomer on a clean Si(001)-(2 × 1) surface (~0.7 eV) [21]. In addition, it was reported that the Si migration is an anisotropic diffusion process that depends on the direction of the surface dimer [22]. Therefore, if reaction (2) is the dominant step, the shape of the oxide/Si boundary should fluctuate. As we can see in Figs. 1(b) and 1(c), the oxide was uniformly removed, so reaction (2) is not the limiting step. Consequently, reactions (3) and (4) are a suitable explanation of the decomposition property. Assuming that the supply of Si monomer to the oxide/Si boundary is sufficient and that the Si monomer can react with the oxide without SiO adsorbate, the SiO adsorbate formed by reaction (3) can restrict reaction (4). In this case, dW/dt can be expressed as

$$\frac{dW}{dt} \propto \frac{k_3 k_4}{k_3 + k_4}, \tag{2}$$

where k_3 and k_4 are the rates of reaction (3) and reaction (4), respectively, and are the thermally activated processes. The fitting curve using Eq. (2) in Fig. 3 for the 650 °C-oxide layer is in good agreement with the measured results. It is natural for the E_d of this fitting curve to be 1.7 and 4.0 eV. This result indicates that two rate-limiting steps [reactions (3) and (4)] are suitable for explaining the observed decomposition property.

The dependence of the decomposition rate on the oxidation temperature (Fig. 3) gives us the information about the related reaction steps to 1.7 and 4.0 eV. When the oxide layer was grown at a lower temperature (470 °C-oxide), the 1.7-eV region extended farther into the lower temperature region. This result indicates that the limiting step in this lower temperature region is altered by the structural change in the oxide layer. As a reference, we show the Si $2p$ chemical shift intensities of XPS spectra, Si^{2+}, Si^{3+}, and Si^{4+}, normalized by Si^{0+} intensity (Table I). This result indicates that the lower-temperature oxide includes slightly larger amounts of the defect (Si^{2+} and Si^{3+}) compared with the higher-temperature oxide, even though the all oxide layers were estimated to be roughly the same thickness (~0.3 nm). On the other hand, the reaction (3) is thought to be affected by the structural change, because this reaction needs to break the SiO_2 network. Therefore, when the oxide layer includes a large amount of the defect, reaction (3) is promoted, and reaction (4) becomes the rate-limiting step. Judging from the above discussion, 1.7 eV could correspond to reaction (4), and consequently, 4.0 eV could be the E_d of reaction (3). In addition, as we can see in Fig. 3, the 725 °C and the 800 °C oxide layers have lower decomposition rates compared with the 650 °C oxide layer, even though they are in the same 4.0 eV region. This result suggests that the crucial oxide structure

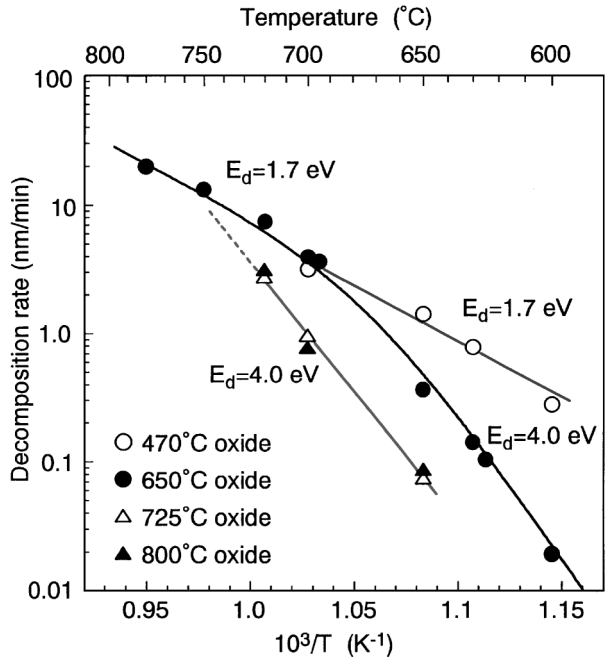

FIG. 3. Arrhenius plot for the decomposition rates of the four types of ultrathin Si oxide layers.

TABLE I. Si $2p$ chemical shift intensities Si^{2+}, Si^{3+}, and Si^{4+}, obtained from the ultrathin Si oxide layers grown at various oxidation temperatures.

Oxidation temperature (°C)	$\frac{Si^{2+}}{Si^{0+}}$	$\frac{Si^{3+}}{Si^{0+}}$	$\frac{Si^{4+}}{Si^{0+}}$
470	0.050	0.051	0.047
650	0.043	0.051	0.067
725	0.045	0.045	0.083
800	0.044	0.046	0.082

for restricting reaction (3) is not the whole oxide layer, but some part of the structure such as a complete SiO_2 (Si^{4+}).

1.7 eV for the SiO desorption is close to the 2 eV reported by Liehr *et al.* for void expansion in a thick SiO_2 layer under UHV annealing (1000–1175 °C) [16]. In addition, it was presented that etching of a clean Si surface under low pressure of oxygen shows 1.5–2.0 eV [12–14]. These experiments are considered to evaluate the final SiO desorption. Moreover, recent first-principle calculations suggest that E_d of the SiO desorption from an O/Si(001) surface including a single missing-atom vacancy is 2.2 eV [23]. This result is reasonable, because in our case, many vacancies could have been formed on the clean Si surface. On the other hand, other experiments, using temperature programmed desorption [6], modulated molecular beam technique [9,10], and optical second-harmonic generation [14] gave higher values of E_d ($>$3.0 eV). This energy could be associated with reaction (1) or (3). Johnson and Engel reported that void expansion in an ultrathin oxide layer is limited by reaction (1) (they used scanning electron microscopy) [7]. This discrepancy compared with our result suggests that the rate-limiting steps could also be influenced by another factor, for example, by the ratio of the Si window area to its perimeter.

In conclusion, we found that thermal decomposition of an ultrathin Si-oxide layer around a Si(001)-(2 $\times$ 1) window that was opened by EB-STD follows two rate-limiting steps that depend on the oxide structure. One step is the reaction of the Si monomer with the Si oxide ($E_d = 4.0$ eV), and the other is the desorption of volatile SiO into the vacuum ($E_d = 1.7$ eV).

The authors thank Dr. Kozo Mochiji, Dr. Alexander A. Shklyaev, Dr. Toshihiro Uchiyama, and Motoshi Shibata of JRCAT for their helpful discussions. This work was performed under the management of a technological research association, the Angstrom Technology Partnership (ATP) in the Joint Research Center for Atom Technology (JRCAT) supported by the New Energy and Industrial Technology Development Organization (NEDO).

*Present address: Fundamental Research Laboratories, NEC Corporation, 34 Miyukigaoka, Tsukuba, Ibaraki 305-8501, Japan.

[1] T. Morimoto *et al.*, in *Extended Abstracts of the 1991 International Conference on Solid State Devices & Materials, Yokohama, 1991* (Business Center for Academic Societies Japan, Tokyo, 1991), p. 23.
[2] S. Fujita, S. Maruno, H. Watanabe, and M. Ichikawa, Appl. Phys. Lett. **69**, 638 (1996); H. Watanabe *et al.*, Appl. Phys. Lett. **70**, 1095 (1997).
[3] G. W. Rubloff, K. Hofmann, M. Liehr, and D. R. Young, Phys. Rev. Lett. **58**, 2379 (1987).
[4] N. Miyata, H. Watanabe, and M. Ichikawa, J. Vac. Sci. Technol. B **17**, 978 (1999).
[5] R. Tromp, G. W. Rubloff, P. Balk, and F. K. LeGoues, Phys. Rev. Lett. **55**, 2332 (1985).
[6] Y. K. Sun, D. J. Bonser, and T. Engel, Phys. Rev. B **43**, 14 309 (1991).
[7] K. E. Johnson and T. Engel, Phys. Rev. Lett. **69**, 339 (1992); Surf. Sci. **290**, 213 (1993).
[8] Y. Wei, M. Wallace, and C. Seabaugh, Appl. Phys. Lett. **69**, 1270 (1996).
[9] J. R. Engstrom and T. Engel, Phys. Rev. B **41**, 1038 (1990).
[10] U. Memmert and M. L. Yu, Surf. Sci. **245**, L185 (1991).
[11] M. L. Yu and B. N. Eldridge, Phys. Rev. Lett. **58**, 1691 (1987).
[12] Y. Ono, M. Tabe, and H. Kageshima, Phys. Rev. B **48**, 14 291 (1993).
[13] A. A. Shklyaev, M. Aono, and T. Suzuki, Phys. Rev. B **54**, 10 890 (1996).
[14] J. B. Hannon, M. C. Bartelt, N. C. Bartelt, and G. L. Kellogg, Phys. Rev. Lett. **81**, 4676 (1998).
[15] M. B. Raschke, P. Bratu, and U. Höfer, Surf. Sci. **410**, 351 (1998).
[16] M. Liehr, J. E. Lewis, and G. W. Rubloff, J. Vac. Sci. Technol. A **5**, 1559 (1987).
[17] H. Watanabe and M. Ichikawa, Rev. Sci. Instrum. **67**, 4185 (1996).
[18] S. Fujita, H. Watanabe, S. Maruno, and M. Ichikawa, Appl. Phys. Lett. **71**, 885 (1997); H. Watanabe *et al.*, Phys. Rev. Lett. **80**, 345 (1998).
[19] N. Miyata, H. Watanabe, and M. Ichikawa, Appl. Phys. Lett. **72**, 1715 (1998); Phys. Rev. B **58**, 13 670 (1998).
[20] K. Fujita, H. Watanabe, and M. Ichikawa, J. Appl. Phys. **83**, 4091 (1998).
[21] Y. M. Mo, J. Kleiner, M. B. Webb, and M. G. Lagally, Phys. Rev. Lett. **66**, 1998 (1991).
[22] B. S. Swartzentruber, Phys. Rev. Lett. **76**, 459 (1996).
[23] T. Uchiyama, T. Uda, and K. Terakura (private communication).